Pore-Resolved NMR Porosimetry

Russell S. Drago,* Donald C. Ferris, and Douglas S. Burns

Contribution from the Department of Chemistry, University of Florida, Gainesville, Florida 32611-7200

Received August 12, 1994[⊗]

Abstract: For the first time, high-field FT-NMR spectra of an adsorbate inside a porous solid exhibits multiple resonances corresponding to different sites. Frequency shift, T_1, and T_2 measurements as a function of adsorbate concentration support the assignment of these resonances to probe molecules in solution and in pores of various sizes within the solid. Resolution of the bands and combination of the NMR intensities with the adsorption isotherm lead to an unprecedented amount of detail about the distribution of the adsorbate in the solid pores as a function of probe concentration (see Figures 5 and 6). The detection of separate resonances by NMR is referred to as pore-resolved NMR porosimetry to distinguish this method from NMR analyses based on extracting information from a single resonance of an adsorbed probe molecule.

Introduction

The adsorptive properties of porous materials have been employed to separate and purify liquids and gases. Recent work from this laboratory has shown the advantage of porous solids when used as catalyst supports.[1] For these applications a fundamental understanding of gas-solid and liquid-solid equilibria is relevant. Investigations of gas-solid equilibria in porous carbonaceous adsorbents showed that the adsorption isotherms required different equilibrium processes involving surface adsorption and multilayer adsorption to fit the data.[2] This work was later extended to investigate the competitive adsorption of probe molecules from dilute solutions.[3]

In all of the above work, the process at low adsorbate concentrations is attributed to surface adsorption in the smaller pores. Pores in supports have been divided into three groups by IUPAC. Micropores are those pores that are <20 Å in diameter. Mesopores are those that are between 20 and 500 Å in size. Macropores are defined as pores with diameters larger than 500 Å.[4] Micropores adsorb molecules with significantly larger adsorption energies than do meso- or macropores due to superimposed interaction potentials from opposite surfaces within the pore.[5,6] Everett and Powl[7] calculated interaction energies as a function of pore size based on the Lennard-Jones potential model. In cylindrical pores of sizes that are five adsorbate diameters or less, the model predicts increasing adsorption energies with decreasing pore size. Preferential micropore adsorption occurs because of these higher adsorption energies.

The above studies employed the classical method for characterizing porous materials through the use of adsorption isotherms. This technique only provides information about the number of different processes required to describe the isotherm. In order to better understand the adsorptive properties of these solids, it would be useful to have a spectral measure of the distribution of the probe in the various micro-, meso-, and macropores at various probe concentrations. This work describes an NMR method that leads to a direct observation of the role of the various pores of carbonaceous adsorbents in the preferential adsorption of one component from a dilute binary solution.

Nuclear magnetic resonance (^{1}H-NMR) has been used extensively to investigate solid-solute interactions. In early work, two ^{1}H-NMR signals were reported for water in contact with Dowex 50W ion-exchange resin.[8] One peak was shown to be exterior water while the second peak was water inside the resin. ^{1}H-NMR has also been used[9] to study water in various hydrated aluminas. The NMR line widths of the protons were a function of surface area as measured by N_2 adsorption and the fraction of hydroxyl groups on the surface could be estimated from the width of the ^{1}H-NMR lines. A series of gels and macroreticular (highly ordered) ion-exchange resins[10,11] in water showed in all cases only a single broad peak for water in the resin and a second peak for external water. Broadened resonances corresponding to only a single interior site for probe molecules adsorbed by carbons have been reported.[12]

The last decade has seen the report of a large body of work using ^{129}Xe, ^{2}H, and proton NMR.[13] The xenon probe experiences large shifts that are very sensitive to the xenon environment.[14,15] The majority of the research in this area involves study of zeolites, silica gel, and porous glasses.[14] Recent reports describe extensions of xenon NMR to porous carbonaceous

[⊗] Abstract published in *Advance ACS Abstracts*, June 15, 1995.

(1) (a) Grunewald, G. C.; Drago, R. S. *J. Mol. Catal.* **1990**, *58*, 227. (b) Grunewald, G. C.; Drago, R. S.; Clark, J. L.; Llvesey, A. B. *J. Mol. Catal.* **1990**, *60*, 239. (c) Grunewald, G. C.; Drago, R. S. *J. Am. Chem. Soc.* **1991**, *113*, 1636. (d) Petrosius, S. C.; Drago, R. S. *J. Chem. Soc., Chem. Commun.* **1992**, 334. (e) Petrosius, S. C.; Drago, R. S.; Young, V.; Grunewald, G. C. *J. Am. Chem. Soc.* **1993**, *115*, 6131.

(2) Drago, R. S.; Burns, D. S.; Lafrenz, T. J. *J. Phys. Chem.* Submitted for publication.

(3) Drago, R. S.; Burns, D. S.; Gregory, T. K. In preparation.

(4) (a) Sing, K. S. W.; Everett, D. H.; Haul, R. A. W.; Moscou, L.; Pierotti, R. A.; Rouquérol, J.; Siemieniewsky, T. *Pure Appl. Chem.* **1985**, *57* (4), 603. (b) Rouquérol, J.; Avnir, D.; Fairbridge, C. W.; Everett, D. H.; Haynes, J. H.; Pernicone, N.; Ramsay, J. D. F.; Sing, K. S. W.; Unger, K. K. *Pure Appl. Chem.* **1994**, *66* (8), 1739.

(5) Everett, D. H.; Whitton, W. I. *Proc. R. Soc. London* **1955**, *A230*, 91.

(6) Farrell, J.; Reinhard, M. *Environ. Sci. Technnol.* **1994**, *28*, 53.

(7) Everett, D. H.; Powl, J. C. *J. Chem. Soc., Faraday Trans. 1* **1976**, *72*, 619.

(8) Gordon, J. E. *J. Phys. Chem.* **1962**, *66*, 1150.

(9) (a)Pearson, R. M. *J. Catal.* **1971**, *23*, 388. (b) Baker, B. R.; Pearson, R. M. *J. Catal.* **1974**, *33*, 265.

(10) Frankel, L. S. *J. Phys. Chem.* **1971**, *75*, 1211 and references cited therein.

(11) (a) Creekmore, R. W.; Reilly, C. N. *Anal. Chem.* **1970**, *42*, 570. (b) Creekmore, R. W.; Reilly, C. N. *Anal. Chem.* **1970**, *42*, 725.

(12) Gradsztajn, S.; Conard, J.; Benoit, H. *J. Phys. Chem. Solids* **1970**, *31*, 1121.

(13) (a) Smith, D. M.; Davis, P. J. in *Characterization of Porous Solids II*; Rodriguez-Reinoso, F., Unker, K. K., Eds.; Elsevier Science Publishers B.V.: Amsterdam, 1991; p 301. For a good review see: (b) Klinowski *J. Chem. Rev.* **1991**, *91*, 1459. (c) Bahceli, S.; Al-Kaisi, A. R. S.; Strange, J. H. In ref 13a, p 293.

0002-7863/95/1517-6914$09.00/0

materials.[15] In all of these studies a single resonance is observed for the adsorbed probe molecule. Low-field FT-NMR and magnetic resonance imaging have also been employed[16] to give pore size information on silica gels and porous glasses.

In the work that will be described here, it will be shown that for the first time a conventional high-field FT-NMR procedure gives rise to multiple signals for an adsorbate inside different size pores of a solid adsorbent. Exchange of the adsorbate between the different pores, as well as between the solution and the solid pores, is shown to be slow on the NMR time scale. Integration of the signals provides quantitative information about the distribution of the probe in the pores of the solid.

Experimental Section

Materials. Probes and solvents were acetonitrile, dichloromethane, benzene, and carbon tetrachloride. All liquids were freshly distilled and stored over 4 Å sieves to prevent contamination from H_2O.

Ambersorb 572 (lot 2125) (A-572) was provided to us by Rohm and Haas Company (Philadelphia, PA) as 1 mm diameter beads. The beads were soxhlet extracted with methanol for 12−24 h, dried in a vacuum-oven overnight at higher than 110 °C, and stored in a capped vial. The same results were obtained when higher temperatures (200 °C) are used to dry the beads. When wet beads are used in an NMR experiment, water is displaced and appears as a separate resonance at low field. Addition of water increases the intensity of this peak. The solids were periodically placed in the vacuum-oven overnight to insure that water was not picked up during handling and standing.

NMR Measurements. Approximately 0.22 g of A-572 was precisely measured into a standard NMR tube. A 1.00-mL aliquot of a known concentration of probe in CCl_4 was then pipeted over the solid. The entire sample was shaken vigorously and allowed to settle and equilibrate for 1 day with occasional agitation unless otherwise noted. The tube was tapped until no trapped air was evident in and around the beads. The ^{1}H-NMR spectrum of the solution inside and surrounding the solid was then obtained using a Varian-300 MHz NMR instrument. The tube was filled so that the solid filled the probe coil. The sweep width was set to 12 000 Hz with the placement of 0 ppm set by an external lock. In all spectra, 256 transients were acquired and the sample tube was not spinning unless otherwise noted. All spectra were obtained at ambient pressure and unless otherwise noted at ambient temperature.

The spectra contain overlapping peaks and these were resolved into individual components to determine peak areas. The spectra were digitized using the program UN-PLOT-IT.[17] The spectra were deconvoluted using Lorentzian curves and a linear base line with the program PeakFit.[18] Various initial estimates of the amplitude, frequency shift, and peak widths converged to the same final spectra. Validity of the fitting procedure is provided by the constancy of the frequency components comprising a series of very different shaped spectra at different concentrations (see Figure 2).

The T_1 relaxation times were measured using the standard procedure.[19] These measurements were made on all samples studied. Measurements at several frequencies in a given resolved band produced the same T_1 within experimental error as those measured and reported at the resolved band maximum. This is not unexpected in view of the similarity of the T_1's for micro- and mesopores.

The T_2 relaxation times (s) were approximated by converting the half width at half height of the curve resolved peaks ($w_{1/2}$, ppm) to seconds using eq 1. Temperature dependent studies indicate the system is the fast exchange region where eq 1 is applicable.[20,21]

$$T_2 = \frac{1}{\pi w_{1/2}\,(300\ \text{MHz})} \tag{1}$$

Adsorption Measurements. The equilibrium acetonitrile solution concentrations were quantified using a Hewlett-Packard HP 5890 A-FID gas chromatograph outfitted with an RSL-160 30 m × 0.32 mm id capillary column from Alltech. The equilibrium concentrations of the benzene solutions were determined from UV/vis spectra (λ = 260 nm) in 0.1-cm quartz UV cells in a Perkin-Elmer Lambda 6 UV/VIS spectrophotometer.

The total number of moles of probe adsorbed per gram of A-572, n, was calculated using eq 2 where C_i is the initial probe concentration (mol/L), C_{eq} is the equilibrium probe concentration (mol/L), V is the volume of solution added (mL), and m is the mass of adsorbent (g).

$$n = \frac{(C_i - C_{eq})V(0.001\ \text{L/mL})}{m} \tag{2}$$

Total adsorption isotherms were obtained by plotting n vs C_{eq}. Best fit curves were drawn through the total adsorption isotherm. Contributions to the adsorption isotherms from the different pores were obtained by multiplying the curve resolved fractional peak area by the total moles of probe adsorbed, n_{total}, as shown in eq 3. The value of n_{total} was the n from the best fit line to eq 2.

$$n_{pore} = \frac{\text{Area}_{pore}}{\text{Area}_{total}}\,(n_{total}) \tag{3}$$

Results and Discussion

Adsorbents, Adsorbates, and Solvent. N_2 porosimetry was carried out on the carbonaceous adsorbent A-572 to afford a comparison to other materials. The results are summarized in Table 1. The plot of pore volume distribution was bimodal with very few pores in the 40−100 Å region. The large mesopore−macropore range encompassed a range of 100−900 Å with the maximum at ≈580 Å. These results should be considered in the context of recent reports discussing the inadequacy of the BET method for microporous solids.[15]

Table 1. N_2 Porosimetry of A-572[a]

surface area (m^2/g)	1160
pore volume (mL/g)	
micropore	0.43
mesopore	0.28
macropore	0.21

[a] The solids were characterized as follows: Surface area and pore volume data were obtained from the N_2 isotherm at 77 K using a Micromeritics ASAP 2000 instrument. Surface areas were determined using a five-point Brunauer−Emmett−Teller (BET) calculation. Micropore volumes were determined using the Harkens−Jura t-plot model with thickness parameters from 3.5 to 5 Å. The Barrett−Joyner−Halerda (BJH) adsorption curve was used for calculating meso- and macropore volumes. Macropore volumes are determined by difference. All calculations were carried out as described in the Micromeritics ASAP 2000 instrument manual.

(14) (a) Ito, T.; Fraissard, J. *J. Chem. Phys.* **1982**, *76*, 5225. (b) Ripmeester, J. A. *J. Am. Chem. Soc.* **1982**, *104*, 289. (c) Reisse, J. *Nouv. J. Chem.* **1986**, *10*, 665. (d) Scharpf, E. W.; Crecely, R. W.; Gates, B. C.; Dybowski, C. *J. Phys. Chem.* **1986**, *90*, 9. (e) Demarquay, J.; Fraissard, J. *Chem. Phys. Lett.* **1987**, *136*, 314. (f) Fraissard, J. *Z. Phys. Chem.*, **1988**, *269*, 657. (g) Ito, T.; Bonardet, J. L.; Fraissard, J.; Nagy, J. B.; Andre, C.; Gabelica, Z.; Derouane, E. G. *Appl. Catal.* **1988**, *43*, L5. (h) Heink, W.; Kärger, J.; Pfeifer, H.; Stallmach, F. *J. Am. Chem. Soc.* **1990**, *112*, 2175.

(15) (a) Foley, H. C.; Bansal, N.; Lafyatis, D. S.; Dybowski, C. *Prep. Am. Chem. Soc., Div. Pet. Chem.* **1991**, *36*, 502. (b) Bansal, N.; Foley, H. C.; Lafyatis, D. S.; Dybowski, C. *Catal. Today*, **1992**, *14*, 305. (c) Saito, A.; Foley, H. C. *AICHE J.* **1991**, *37*, 429.

(16) (a) Smith, D. M.; Davis, P. J. In ref 13a, p 301. (b) Ewing, B.; Davis, P. J.; Majors, P. D.; Drobbny, G. P.; Smith, D. M.; Earl, W. L. In ref 13a, p 709. (c) Glaves, C. L.; Brinker, J.; Smith, S. M.; Davis, P. J. *Chem. Mater.* **1989**, *1*, 34. (d) Gallegos, D. P.; Smith, D. M. *J. Colloid Interface Sci.* **1987**, *119*, 127.

(17) Silk Scientific Inc., P.O. Box 533, Orem, UT 94912.

(18) Jandel Scientific Inc., P.O. Box 7005, San Rafael, CA 84059.

(19) Varian VXR-300 User Manual.

(20) Drago, R. S. *Physical Methods in Chemistry*; W. B. Saunders Publishing: Philadelphia, PA. 1992.

(21) Drago, R. S.; Hirsch, M. S.; Ferris, D. C.; Chronister, C. W. *J. Chem. Soc. Perkin Trans. 2*, **1994**, 219.

Table 2. Summary of Solutes and CCl_4 and Physical Properties[a]

probe liquid	mw (g/mol)	polarizability[b] (Å^3)	dipole moment (D)	molar volume (mL/mol)	ΔH_v (kcal/mol)	S' [c]	T_1[d] (s)	δ[d] (ppm)
CH_3CN	40.05	4.40	3.92	52.2	7.3	3.00	4.25	2.15
C_6H_6	78.11	10.3	0	89.4	7.35	1.73	4.91	7.29
CH_2Cl_2	84.93	6.48	1.60	64.0	6.74	2.08	5.29	5.32
CCl_4	153.82	10.5	0	96.5	7.12	1.49		

[a] *Lange's Handbook of Chemistry*, 13th ed.; McGraw-Hill: New York, 1985. All data are from this source unless otherwise specified. [b] *Handbook of Chemistry and Physics*, 71st ed.; CRC Press: Boca Raton, FL, 1991. [c] See reference 21. [d] Obtained from this work. In CCl_4 solution relative to internal TMS.

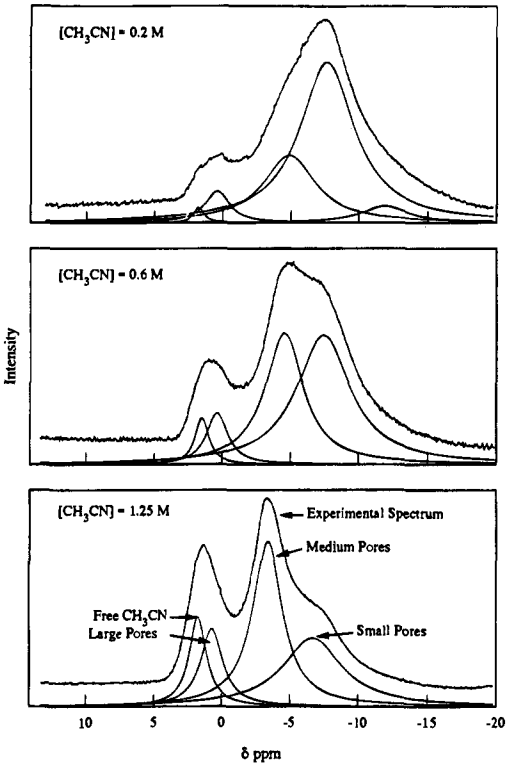

Figure 1. ^{1}H NMR spectra of CH_3CN in CCl_4 over A-572. Initial solution probe concentrations are shown. The intensity scale increases with increased probe concentration.

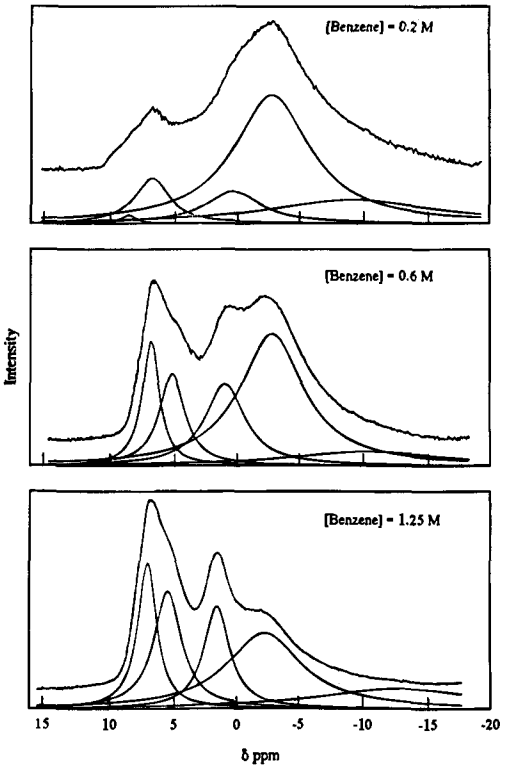

Figure 2. ^{1}H NMR spectra of benzene in CCl_4 over A-572. Initial solution probe concentrations are shown.

In this study, the distributions of three probe molecules between the carbonaceous adsorbent and solutions in carbon tetrachloride were studied by ^{1}H-NMR. Since CCl_4 is a nonpolar, poorly solvating solvent, solute–solvent interactions are minimized and the CCl_4–solid dispersion interactions remain constant when the probe is changed. Therefore, we are able to compare the donor, acceptor, dispersion, and polarity properties which influence the adsorption potential of the different probes. Using CCl_4 as the solvent has the added advantage that no protons interfere with the ^{1}H-NMR spectrum of the probe molecule. In addition, each probe only has equivalent protons producing a singlet in the solution ^{1}H-NMR spectrum. The relevant physical properties of the probes and solvent are summarized in Table 2.

Qualitative ^{1}H-NMR Analysis. The ^{1}H-NMR spectra for 0.2, 0.6, and 1.2 M solutions of acetonitrile, benzene, and dichloromethane in CCl_4 solutions inside and surrounding the carbonaceous adsorbent, A-572, are presented in Figure 1–3. The resolution of the spectra into the minimum number of components required to fit the observed spectra is also illustrated by the smooth solid lines. It should be emphasized that the intensities are relative and the absolute intensity increases with increasing concentration of each probe. For this reason, the small peak at highest field disappears at high concentration. Furthermore, CH_2Cl_2 has fewer protons per unit volume of solvent and gives a smaller signal-to-noise ratio than the other probes. This leads to difficulty in separating the large pore and solution resonances in the more concentrated solution. In the most dilute solution, the peak observed at lowest field is assigned to CH_2Cl_2 in the largest pores. A summary of the frequency shift, T_1, and T_2 values for the resolved signals of the three adsorbed probes is given in Table 3 along with the peak assignments (vide infra). It is significant to note that the difference in the frequency shift of the free and large pore resonances is 1.4 ± 0.4 ppm for all three probes. The free and the medium pore resonances differ by 5.9 ± 0.5 ppm for all three probes. The free and less shifted small pore resonances differ by 9.6 ± 0.3 ppm. Since acetonitrile and benzene are common donor molecules and CH_2Cl_2 is a common acceptor molecule,[22] these results suggest that the solid environment and not donor–acceptor interactions gives rise to the shifts. This conclusion is in agreement with literature[10,12] interpretation of the broadening mechanism.

The observation of separate resonances in the NMR indicates that the exchange of molecules between the sites corresponding to these resonances is slow on the NMR time scale. This is confirmed by the temperature independence of the spectra over 20 to 60 °C and the absence of off-diagonal peaks in a COSY spectrum accumulated for 8 h. Thus, the rate of exchange between pores is slowed by the probe access to the pores from

(22) Drago, R. S. *Applications of Electrostatic-Covalent Models in Chemistry*; Surfside Scientific Publishing: P.O. Box 13413, Gainesville, FL 32604, 1994.

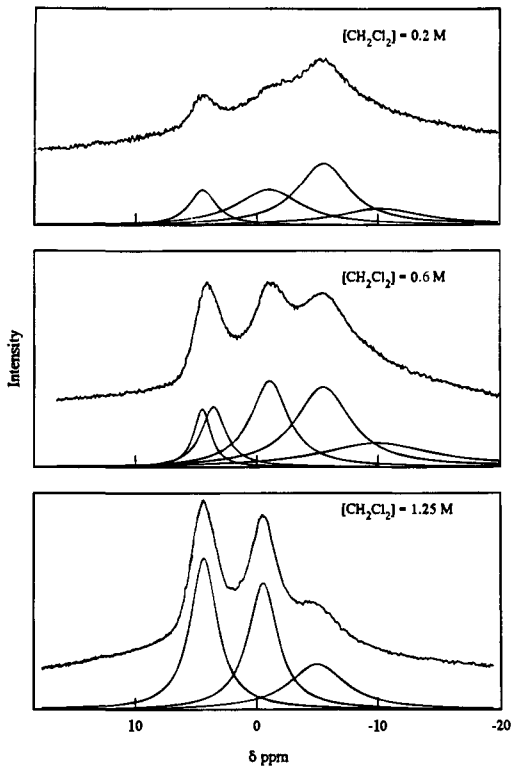

Figure 3. ^{1}H NMR spectra of CH_2Cl_2 in CCl_4 over A-572. Initial solution probe concentrations are shown.

Table 3. Peak Assignments for Adsorption of 0.6 M Probes from CCl_4 by A-572

probe	peak shift (ppm)	T_1 (s)	$10^4\ T_2{}^b$ (s)	assignment
CH_3CN	1.9	1.5	18	"free"
	0.4	1.5	11	large pores
	−4.6	0.4	6.3	medium pores
	−7.5	0.3	4.4	small pores
	−11.9[a]	0.3		
benzene	6.9	2.1	13	"free"
	5.2	1.5	8.8	large pores
	1.0	0.6	5.6	medium pores
	−2.7	0.7	3.5	small pores
	−10.5	0.6	1.4	
CH_2Cl_2	4.4	1.0	12	"free"
	3.5	0.7	8.8	large pores
	−1.0	0.3	5.8	medium pores
	−5.5	0.1	3.9	small pores
	−10.0	0.1	1.9	

[a] From C_i = 0.2 M CH_3CN experiment. [b] The NMR spectra are temperature independent over the range 20−60 °C suggesting the system is in the fast motional narrowing limit.

solution. The different frequency shift, T_1, and T_2 values for the same probe molecule inside the porous solid arise from fast exchange of weakly bound surface molecules with those in the liquid-like multilayer of the different size probes. Acetonitrile in the micropores will have a larger shift and shorter T_1 and T_2 than acetonitrile in the macropores because the averaging in the micropores involves a greater fraction of surface-bound physisorbed molecules than the averaging in the macropores. As the pore becomes larger, the averaging involves fewer surface-bound molecules and the shifts, T_1, and T_2 approach those of the liquid. This interpretation leads to the assignment of the upfield peaks to probe in the smallest pores. The downfield peak arises from probe in the large pores and the middle peak from probe in the medium pores.

The quantitative interpretation of the magnitudes of the shifts, T_1, and T_2 is complicated by the inhomogeneity of surface and pore volumes which comprise the micropores, mesopores, or macropores. Surface sites of different binding strength would, under fast exchange conditions, average in different δ, T_1, and T_2 values. If there were any strong binding sites that do not exchange, they would not be detected in the NMR. The distribution of pore volumes contributing to the peak assigned to each small pore, medium pore, or large pore also influences δ, T_1, and T_2. Each peak is comprised of overlapping components with slightly different ratios of surface bound and multilayer probe molecules. The inhomogeneity of surface sites and pore volumes does not impact on the conclusions to be drawn, and is implied in our use of the terms micropore, mesopore, and macropore volumes. The novel aspect of the NMR spectra obtained in this study is the demonstration of gaps in the spectra which correspond to low concentrations or no pores of certain dimensions. This permits an easily measured, unambiguous view of the role of these pores in the adsorption process. The concentration dependence of the spectra for acetonitrile, benzene, and methylene chloride will be seen to provide further support for the spectral assignments.

Concentration Dependence of the Acetonitrile Spectra. The high-resolution ^{1}H-NMR spectrum of acetonitrile as the probe molecule in CCl_4 in contact with A-572 is shown in Figure 1. The observation of separate peaks for different pores indicates that the exchange of probe molecules from one type of pore to another must be slow on the NMR time scale. Temperature variation showed little change in the NMR spectrum over the range of 20 to 60 °C indicating that interpore exchange makes no contribution to the line width and that the width is dominated by intrapore exchange. The experimental spectrum consists of two very broad signals with shoulders which curve resolve into 4 or 5 smaller signals. Though significant changes in the spectra occur with probe concentration, it is gratifying that curve resolution gives, for all the spectra of a given probe, peaks with about the same frequency shifts that differ mainly in their relative intensities. The frequency shifts, T_2's, and relative areas of the resolved peaks as a function of probe concentration are given in Table 4 for the three probes. The peak assignments are borne out by the concentration-dependent studies shown in Figure 1. The downfield peak in the acetonitrile spectra is resolved into two components. The sharper component and more downfield peak in each resolved spectrum (1.9 ppm) appears where expected for acetonitrile in solution and is assigned to "free" acetonitrile in the bulk CCl_4 solution surrounding the solid. The slightly broader component, upfield by about 1.4 ppm from the solution CH_3CN resonance, is assigned to probe molecules in the large pores. These "large pores" probably include macropores and large mesopores of the adsorbent. Since these pores are quite large, most of the molecules in a given pore are in an environment similar to that in solution. As a result, this signal is shifted the least, T_2 is similar to that of the solution peak in the sample, and little change is observed in T_1. The concentration dependence of the intensity of this peak is consistent with this assignment. The relative intensity of this peak continues to increase with probe concentration at all concentrations employed.

The second large, broad up-field peak contains shoulders indicating that there are actually two or possibly three peaks under a common envelope. Curve resolution of the 0.2 M spectrum places the peaks at −4.8 and −7.6 ppm with a contribution from a peak at −11.9 ppm which is resolved only at low probe concentrations. At low concentration (Figure 1), this broad most upfield peak and a larger peak at −7 ppm develop first. As the CH_3CN concentration is increased over the A-572, the peak at −4 ppm becomes larger than the signal at −7 ppm. The peak at −11.9 ppm in the 0.2 M solution is masked by the peak at −7 ppm at higher probe concentrations.

Table 4. Summary of Frequency Shifts, T_2's, and Relative Areas from ^{1}H-NMR

probe	conc (M)	frequency shift (ppm)	10^4 T_2 (s)	relative area (%)
CH_3CN	0.2	1.9	24	1.2
		0.4	9.8	5.8
		−4.8	4.6	25.1
		−7.6	4.4	62.5
		−11.9	5.1	5.5
	0.6	1.9	18	4.9
		0.4	11	8.2
		−4.6	6.3	37.1
		−7.4	4.4	49.8
	1.25	1.8	14	13.1
		0.3	11	14.4
		−4.4	8.1	41.0
		−6.7	4.1	31.5
benzene	0.2	8.6	16	0.8
		6.9	6.8	9.9
		0.3	3.8	11.2
		−2.7	3.5	59.1
		−9[a]	1.2	19.0
	0.6	6.9	13	12.5
		5.2	8.8	13.5
		1.0	5.6	18.5
		−2.7	3.5	46.4
		−11[a]	1.4	9.1
	1.25	7.1	12	17.4
		5.5	8.0	20.7
		1.6	8.5	16.9
		−2.3	3.0	32.8
		−14[a]	1.4	12.1
CH_2Cl_2	0.2	4.4	7.9	12.9
		−1.0	3.4	28.8
		−5.5	4.1	41.7
		−10.3	2.5	16.6
	0.6	4.4	12	8.48
		3.5	8.8	12.2
		−1.0	5.8	26.3
		−5.5	3.9	34.8
		−10.0	1.9	18.3
	1.25	4.3	7.9	40.2
		−0.5	7.3	36.4
		−5.0	3.9	23.4

[a] These peaks are very broad and the frequency shifts are not accurately known.

T_1 measurements indicate that these up-field peaks relax ~4 times faster (≈0.4 s) than the signals assigned to the probe in the solvent and large pores (1.5 s).

The concentration dependence of the T_1 and T_2 values supports the peak assignments. The T_2 value (half width at half height) for the smallest pores (-7 ppm) is nearly the same at all concentrations (4.3×10^{-4} s). This suggests that the micropores are essentially filled at 0.2 M so the fraction of surface-bound molecules to multilayer molecules remains constant in 0.2–1.25 M solutions. Our previous analyses[2,3] also assigned highest adsorption equilibrium constants to surface adsorption within the smallest accessible pores of the solid. On the other hand, the T_2 values for the peak at −4.6 ppm assigned to the medium pores increases from 4.6×10^{-4} to 6.3×10^{-4} to 8.1×10^{-4} s as the concentration is increased from 0.2 to 0.6 to 1.25 M. This is expected behavior for incomplete filling of the mesopores at low concentration. Since the fraction of surface-bound molecules in the pore decreases as the amount of liquid-like CH_3CN in the multilayer is increased, the average T_2 increases and the half width at half height decreases.

The large-pore behavior leads to different spectral changes than adsorption in the medium pores. The T_2 values for the three probes are $10.7 \times 10^{-4} \pm 0.8 \times 10^{-4}$ sec and increase only slightly in going from 0.2–1.25 M CH_3CN. The surface area of the large pores is a very small fraction of the total solid surface area. Therefore, at all probe concentrations the number of surface-bound probe molecules in the large macropores is small compared to the number that are involved in multilayer adsorption. As such, the short T_2 associated with surface-bound CH_3CN has only a small effect on the mole fraction averaged, measured line width. Increasing the CH_3CN concentration up to 3 M shows that the intensities of the small pore and medium pore peaks reach a maximum while the solution and large pore resonances increase in intensity with increasing molarity.

The interpretation of the concentration dependence of the frequency shift parallels that of the T_2 values. Rapid exchange of surface-bound and multilayer molecules produces a mole fraction averaged frequency shift. This leads to the largest upfield shift for molecules in the micropores. There is a slight concentration dependence on the frequency shift for the various pores. The resonance for each pore type is shifted less with increasing concentration, and this is consistent with incomplete filling of the pores at low adsorbate concentration.

All three probes (CH_3CN, C_6H_6, and CH_2Cl_2) give rise to similar differences in the shifts of the solution resonances and that in the different small, medium, or large pores. This dependence on pore size suggests that the shift differences arise from the diamagnetic susceptibility contribution of the solid surface to surface-bound molecules. The mole fraction averaging of this shift and the more liquid-like multilayer shift gives rise to different frequency shifts for different size pores because of the differences in the ratios of multilayer and surface-bound molecules. The diamagnetic contribution is expected to be similar for donor (CH_3CN, C_6H_6) and acceptor (CH_2Cl_2) molecules.[22] The observation of similar shifts for all three probes indicates a minor, if any, donor–acceptor contribution to the shift. This absence could arise from weak donor–acceptor properties for the solid, or from such a small concentration of donor or acceptor sites that their average contribution to the observed shift is negligible. Thus, the principal mechanism leading to the observation of different resonances is the diamagnetic contribution to the surface-bound molecules from the walls of the pores.

The interpretation of the spectra obtained for CH_3CN in A-572 is consistent with the nitrogen porosimetry studies (Table 1) indicating a bimodal distribution of pore dimensions. Gaps exist in which there are few or no pores of intermediate size. The ^{1}H-NMR spectra show three distinct groups of pores. The gap separating the two broad signals corresponds to a group of pores of intermediate size in which few or no pores exist. If there were a continuous distribution in this range of pore dimensions, a single broad peak would result in the ^{1}H-NMR. The NMR explanation given above suggests that in each group of pores, minor changes in the size of the pores would contribute to the width of the observed peaks because the ratio of the surface-bound and multilayer molecules changes with size.

Concentration Dependence of the Benzene Spectra. Figure 2 shows the results for the concentration dependence of the adsorption of benzene by A-572 from CCl_4 solvent. Each spectrum contains two very broad signals similar to that observed for CH_3CN. These two broad signals are also curve resolved into five smaller signals. The sharpest and most downfield signal (7 ppm) has a frequency shift near that expected for benzene in solution and is attributed to benzene in the bulk CCl_4 solution surrounding the solid. The next peak upfield (5.2 ppm) is slightly more broad than the solution signal, and it is assigned to the signal of benzene in the macropores and large mesopores of the solid (large pores). Consistent with the data for CH_3CN, the signal is only slightly shifted with some

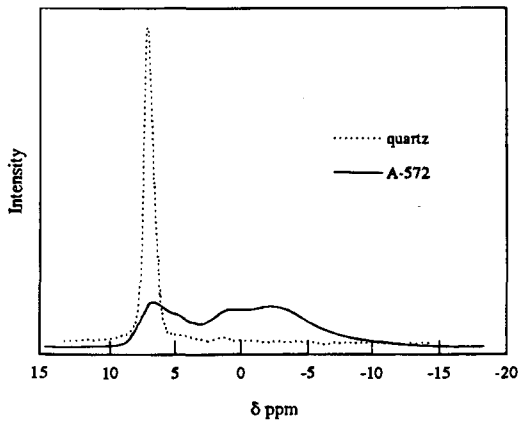

Figure 4. ^{1}H NMR of 0.6 M benzene in CCl_4 in contact with powdered glass.

broadening (T_2 decreases) and little change in T_1 (2.1 s for free; 1.5 s for large pore).

The large, broad upfield peak consists of three curve-resolved signals at 1.0, −2.7, and −10.5 ppm. The concentration dependence spectra for the 1.0 and −2.7 ppm peaks show the same behavior as observed for CH_3CN, and hence the interpretation of the frequency shifts T_1, and T_2 values indicates benzene being preferentially adsorbed by the micropores. The peak at −10.5 ppm is so broad that its maximum cannot be accurately determined.

In order to assess the influence of solid particles on the field homogeneity, a series of experiments were also carried out using quartz obtained from powdering an NMR tube. As shown in Figure 4, the spectrum of 0.6 M benzene in CCl_4 in the presence of the crushed quartz glass does not shift the signal. The signal is broadened from field inhomogeneity associated with not spinning the sample tube. In addition, the T_1 measurements of benzene around the crushed glass gave a value of 4.5 s whether the sample tube is spinning or not. This value is comparable to the solution T_1 value (4.9 s) and more than two times the largest T_1 measured for benzene/CCl_4 surrounding A-572. The observations of smaller T_1 values, increased line widths, and smaller T_2 values for benzene adsorbed by A-572 compared to crushed glass indicate the spectra for the former are not an artifact of the experimental procedure.

Concentration Dependence of the Dichloromethane Spectra. The ^{1}H-NMR spectra of dichloromethane, a hydrogen bonding probe molecule, are presented in Figure 3 and are similar to those of benzene and acetonitrile. The frequency shift, T_1, and T_2 values for the various signals are summarized in Tables 3 and 4. The peak assignments are consistent with those made for benzene and CH_3CN. The upfield peak again is two or three signals at −1.0, −5.5, and −10.0 ppm. The signal at −10.0 ppm is masked by the other peaks at higher concentration, and the peaks at −1.0 and −5.5 ppm grow relative to one another as observed for CH_3CN and benzene with increasing concentration. The downfield peak was curve resolved into two signals for 0.6 M CH_2Cl_2 in CCl_4 in contact with A-572. In the cases of 0.2 and 1.25 M CH_2Cl_2 solution, the free CH_2Cl_2 peak and the macropore peak are not separated. The frequency shift of the macropore resonance is the same as is the resonance for free CH_2Cl_2; however, the T_2 values suggest assignment of a component of the resonance to CH_2Cl_2 in the macropores.

Adsorption−^{1}H-NMR Experiments for Acetonitrile. In order to determine the number of moles of adsorbate in the various pore types, a total adsorption isotherm was measured for adsorption of the probe from CCl_4. In every case, the ratio of volume (1.00 mL) of probe solution to mass (0.220 ± 0.002 g) of A-572 was constant so that adsorption data from all samples could be directly compared. A best fit line was drawn through the total adsorption isotherm in which the total number of moles of probe adsorbed was calculated using eq 2. The curve-resolved areas from ^{1}H-NMR, Table 4, were then used with the best fit isotherm curve to calculate the fraction of probe molecules in each pore type as in eq 3. This procedure presents for the first time a direct measure of the components of the adsorption isotherm by the different pores.

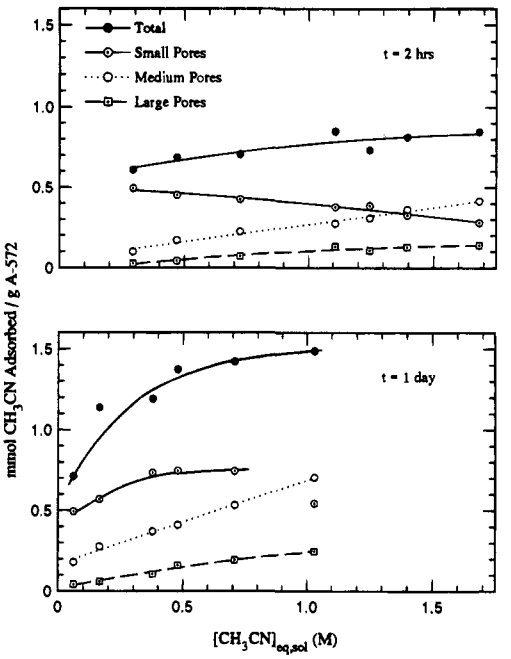

Figure 5. Adsorption of CH_3CN from CCl_4 by the different size pores in A572. Solution equilibrium probe concentrations are given on the abscissa.

Figure 5 shows the adsorption isotherms for adsorption of CH_3CN from CCl_4 by the pores of A-572. Results are presented for samples equilibrated for 2 h and 1 day. The total adsorption capacity is approached at longer time and higher concentrations. The number of moles of CH_3CN adsorbed by the large pores and medium pores increases with adsorbate concentration as expected from the NMR data shown in Figure 1 and with equilibration time. Furthermore, the number of moles of adsorbate in the medium and large pores, for a given equilibrium concentration, increases with time. For example, at C_{eq} = 0.5 M, the number of moles of CH_3CN adsorbed by the large pores increases from 0.05 to 0.15 mmol per gram of A-572 in changing the equilibration time from 2 h to 1 day. The number of moles of CH_3CN adsorbed by the medium pores increases from 0.17 mmol per gram of solid after 2 h to 0.4 mmol per gram of solid after 1 day. The adsorption process involves displacing CCl_4 from pores large enough to hold it.

The data in Figure 5 show that after 1 day of contact at $C_{eq,sol}$ = 0.06 M CH_3CN, 0.71 mmol of CH_3CN were adsorbed per gram of A-572. Of this total amount adsorbed, 0.49 mmol CH_3CN (68%) were adsorbed by the small pores, 0.18 mmol CH_3CN (25%) were adsorbed by the medium pores, and 0.04 mmol of CH_3CN (6%) were adsorbed by the large pores. At $C_{eq,sol}$ from 0.17 to 0.71 M, the number of moles CH_3CN adsorbed by the small pores (0.72 mmoles; 0.038 mL) is relatively constant, whereas the number of moles CH_3CN adsorbed by the medium and large pores increases with increasing equilibrium concentration. Consistent with the 2 h equilibration data, the fraction of CH_3CN molecules adsorbed in the medium pores increases more significantly than in the large pores over this concentration range. This is shown in Figure 5 and Table 4

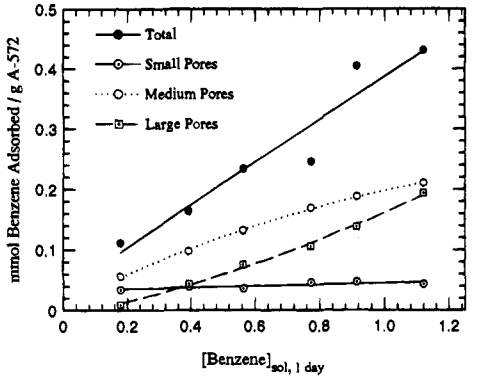

Figure 6. Adsorption of benzene from CCl_4 by the different size pores in A572. Solution equilibrium probe concentrations are given on the abscissa.

where the relative area of the large pore resonance increases from 5.8% to 14.4% ($\Delta\% = 8.6\%$). Over the same concentration range, the relative area of the medium pore resonance increases from 25.1% to 41.0% ($\Delta\% = 15.9\%$).

Although the ^{1}H-NMR spectrum of CH_3CN inside and surrounding A-572 is dependent on changes in bead packing in the NMR tube, these errors do not affect the adsorption studies. In cases where the beads are not packed as tightly, there is more "free solution" surrounding the beads and this signal becomes more intense in the measured spectrum. However, curve resolution of the spectra would give the same values for the relative peak areas for the resonances assigned to the small, medium, and large pores. Since the total amount of probe adsorbed is determined from the adsorption measurement, the amount of probe molecule adsorbed by the different pore types is only dependent on these relative areas.

Consider the adsorption after 2 h of contact time. The capacity of the small pores decreases with increasing concentration. This is not consistent with the NMR conclusion in which the small pores were considered essentially filled even at 0.2 M CH_3CN. At high adsorbate concentrations, in which a significant fraction of the molecules are adsorbed by the medium and large pores, errors associated with the curve-resolution technique of the most shifted resonances of the small pores increases. At low concentrations, a significant portion of the small pore peak area and the total peak area comes from the very broad resonance at -12 ppm. As shown in Figure 1, this signal is not resolved at higher concentration and since it is so broad, some of this peak area may be associated with the signal for the medium pores (-5 ppm). This leads to an underestimation of the small pore adsorption capacity and an overestimation of the medium pore capacity. It is likely that the isotherm for small pore adsorption is constant rather than decreasing with increasing concentration. At an equilibrated concentration of 0.2 M CH_3CN, the small pores are filled.

Adsorption–^{1}H-NMR Experiments for Benzene. Figure 6 presents the adsorption isotherm for benzene from CCl_4 by the pores of A-572. The samples were equilibrated for 1 day. Figure 6 shows the total adsorption isotherm, as well as the adsorption isotherms calculated for each pore type. The total adsorption isotherm indicates that the adsorbent has not reached its capacity for benzene even at the highest concentration studied. This isotherm has a shape similar to one obtained for adsorption of benzene from cyclohexane.[3] Interestingly, the number of moles of benzene adsorbed by the small pores is relatively constant and increases only slightly over the concentration range studied. This is in contrast to the data for CH_3CN in which the isotherm for the small pores decreases with increasing adsorbate concentration. For benzene, the small pore region of the spectrum was curve resolved into two components for all solution concentrations used. In this case, there is no underestimation of the adsorption by the small pores as in the case of CH_3CN. The capacity of the small pores is reached very quickly (0.04 mmol of C_6H_6 per gram of A-572; 0.004 mL). Hence, even at 0.2 M initial benzene concentration, most of the benzene is adsorbed by the medium pores (0.05 mmol of C_6H_6 per gram of A-572). The number of moles adsorbed by the medium pores and large pores increases at the same ratio with increasing benzene concentration up to about $C_{eq,sol} = 0.8$ M. At higher concentrations, the amount of benzene going into the medium pores relative to the large pores decreases as the medium pores become filled to capacity.

The preferential adsorption of benzene from CCl_4 is rationalized as follows. Both have the same polarizability. There are no dipole forces involved in either case. However, in addition to benzene having a larger ΔH_v, it also has a larger solvent polarity parameter, S'.[21] Apparently, the smaller size and shape lead to larger nonspecific interactions.

Conclusions

Frequency shift, T_1, and T_2 data as a function of the amount of adsorbate are used to assign different resonances in the ^{1}H-NMR spectra of adsorbates in porous solids to different-size pores. A procedure is reported whereby an adsorption isotherm can be decomposed into components for different pores. These results (Figures 5 and 6) provide an unprecedented degree of detail about the distribution of adsorbates in the pores of the adsorbent. Preferential adsorption of a probe molecule from a dilute solution in CCl_4 solvent by the small pores occurs first. Upon increasing the probe concentration, the ^{1}H-NMR signals attributed to probe molecules in the small and medium pores reach a maximum, and the signals associated with the large pores and "free" probe increase.

There are several important applications of pore-resolved NMR porosimetry. Our N_2 porosimetry measurements were not able to resolve the pores below 40 Å into the bimodal distribution of pore sizes found by NMR porosimetry. More extensive and expensive software is required to gain this information. Another advantage of NMR porosimetry is that probe molecules of size comparable to those used in practical applications can be used to get a more relevant measure of the adsorptive capacity of the pores in a porous solid. Applications in which pore blockage leads to a bonded adsorbent or dead catalyst can also be studied by pore-resolved NMR porosimetry.

Acknowledgment. The authors acknowledge the support of this research by ARO and ERDEC.

JA9426913